

## THE THERMAL DECOMPOSITION OF $\gamma$ -IRRADIATED LEAD NITRATE BY DYNAMIC THERMOGRAVIMETRY

S M K NAIR and KOSHY KUNJU MALAYIL

*Department of Chemistry, University of Calicut, Kerala 673 635 (India)*

(Received 3 August 1987)

### ABSTRACT

The thermal decomposition of  $\gamma$ -irradiated lead nitrate was studied by thermogravimetry (non-isothermal conditions). The reaction order, activation energy, frequency factor and entropy of activation were computed by means of the Coats–Redfern, Freeman–Carroll, Horowitz–Metzger and the modified Horowitz–Metzger methods. The mechanism for the decomposition follows the Mampel model equation, viz.  $-\ln(1-\alpha)$  for  $g(\alpha)$  and the rate-controlling process is random nucleation with the formation of a nucleus on every particle.

### INTRODUCTION

Several studies on the thermal decomposition of lead nitrate employing thermogravimetric and gas evolution methods have been reported [1–6]. An investigation has also been made on the effect of  $\gamma$ -irradiation on the thermal decomposition of the salt by the gas evolution method over the temperature range 380–425 °C [7]. It has been observed that the irradiation enhances the decomposition rate, the effect increasing with dose. The rate constants in the acceleratory and decay stages are increased. The present paper reports studies on the thermal decomposition of  $\gamma$ -irradiated lead nitrate by thermogravimetry (TG) and the evaluation of the kinetic parameters for the decomposition reaction and elucidation of mechanism of the decomposition reaction.

There has been considerable discussion in the literature concerning the validity of kinetic data obtained by thermal analysis under non-isothermal conditions [8,9]. However, the method has certain advantages also [10]. In the present investigation a non-isothermal method was used.

### EXPERIMENTAL

#### *Material*

GR grade lead nitrate (E Merck) was used in the form of a fine powder (200–240 Mesh). It was dried and stored in vacuo over  $P_2O_5$ .

### *Irradiation*

Samples of the dried salt, sealed in glass ampoules, were irradiated at room temperature with  $^{60}\text{Co}$   $\gamma$ -rays at different doses between 100 and 400 Mrad (dose rate of  $0.2 \text{ Mrad h}^{-1}$ ). The irradiated samples were also kept over  $\text{P}_2\text{O}_5$  before thermal decomposition studies.

### *Estimation of damage*

The nitrite produced in the irradiated samples was estimated spectrophotometrically as reported earlier [11]. A Beckman model DU<sub>2</sub> instrument was used.

### *TG studies*

Non-isothermal mass-loss measurements in air were made using an automatically recording thermal analyser, Ulvac Sinku-Riko (Japan) TA 1500. The heating rate was  $5^\circ\text{C min}^{-1}$  and chart speed was  $4 \text{ mm min}^{-1}$ . In all experiments 10 mg of the sample was taken. The recorded total mass loss in all cases was  $3.3 \pm 0.05 \text{ mg}$ , confirming the formation of PbO as the final product of decomposition. All the data have been normalized to a mass of 100 mg.

## RESULTS

### *The chemical damage*

The concentration of damage  $\text{NO}_2^-$  in the irradiated samples is given below. The concentration of  $\text{NO}_2^-$  increases with irradiation dose.

Dose (Mrad)	100	200	300	400
$\text{NO}_2^-$ (p p m)	2000	2336	2822	3167

### *TG traces*

The thermograms were redrawn, as mass versus temperature (TG) curves and are shown in Fig. 1. All the curves are essentially of the same pattern. The decomposition proceeds in three stages. After the second stage a horizontal level is observed. In the irradiated samples the decomposition proceeds faster in the three stages. Duplicate, and in some cases, triplicate

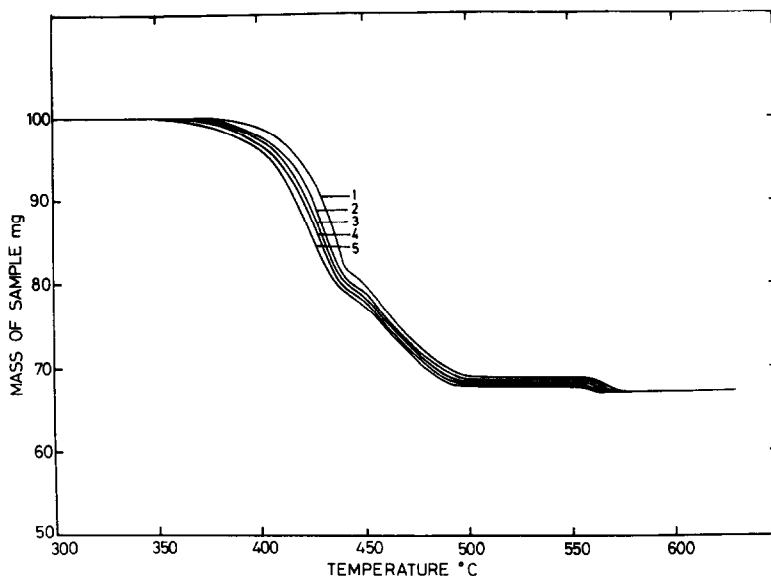


Fig 1 TG curves of lead nitrate (1) unirradiated, (2) irradiated with 100 Mrad, (3) irradiated with 200 Mrad, (4) irradiated with 300 Mrad, (5) irradiated with 400 Mrad

runs were made on all samples with resultant agreement with each other to within about 1%

#### *Evaluation of the kinetic parameters*

Several methods have been employed for the calculation of kinetic parameters from non-isothermal TG data. In the present case, the Coats–Redfern [12], Freeman–Carroll [13], Horowitz–Metzger [14] and the modified Horowitz–Metzger [15] methods are used. The details of the calculation in each case have already been reported [16,17]

##### *The Coats–Redfern method [12]*

According to this method, a plot of either

$$\log\left[1 - (1 - \alpha)^{1-n}/T^2(l - n)\right] \text{ against } 1/T \quad (1)$$

or, where  $n = 1$ ,

$$\log\left[-\log(1 - \alpha)/T^2\right] \text{ against } 1/T \quad (2)$$

where  $\alpha$  is the fraction decomposed,  $n$  is the order of the reaction,  $T$  is the temperature (K) and  $R$  is the gas constant, should result in a straight line of slope  $-E/2.303R$  for the correct value of  $n$

In the present study, eqns (1) and (2) are applied to our data on lead nitrate by the least squares linear regression method. The best correlation is

obtained with eqn (2) for the three stages and therefore the order of the reaction is 1 in both the irradiated and unirradiated samples. The activation energy ( $E$ ) and the frequency factor ( $Z$ ) were calculated from the slope and intercepts, respectively, of the plots. The entropy of activation was calculated using the relation

$$Z = (kT_s/h) \exp(\Delta S/R) \quad (3)$$

where  $k$  is the Boltzmann constant,  $h$  is the Planck constant,  $T_s$  is the peak temperature of decomposition and  $R$  is the gas constant. The values of  $E$ ,  $Z$ ,  $\Delta S$  and the correlation coefficient ( $r$ ) are given in Table 1.

#### *The Freeman–Carroll method [13]*

For a reaction which involves solid state decomposition, the Freeman–Carroll equation is used in the form

$$\Delta \log(dw/dt)/\Delta \log w_r = (-E/2.3R) \Delta(1/T)/\Delta \log w_r + n \quad (4)$$

where

$$dw/dt = (dw/dT) \phi \quad (5)$$

and

$$w_r = w_c - w$$

in which  $\phi$  is the heating rate ( $K \text{ min}^{-1}$ ),  $w$  is the mass loss at time  $t$  and  $w_c$  is the maximum mass loss. For a first-order process the equation assumes the form

$$\log[dw/dt/w_r] = -(E/2.3RT) + \log Z \quad (7)$$

A plot of the left-hand side of eqn (7) versus  $1/T$  was linear for the three stages and  $E$  and  $Z$  were obtained from the slope and intercept, respectively. The value of  $\Delta S$  was calculated as before. Values of  $E$ ,  $Z$ ,  $\Delta S$  and  $r$  are given in Table 1.

#### *The Horowitz–Metzger method [14]*

The Horowitz–Metzger equation applicable to a first-order kinetic process is

$$\log[\log(w_c/w_r)] = E\theta/2.3RT_s^2 - \log 2.3 \quad (8)$$

where  $\theta = T - T_s$  in which  $T$  is the temperature under consideration and  $T_s$  is the peak temperature. A plot of  $\log[\log(w_c/w_r)]$  versus  $\theta$  should be linear, and  $E$  was calculated from the slope. The value of  $Z$  was calculated from the equation

$$E/RT_s^2 = Z/\theta \exp(-E/RT_s) \quad (9)$$

The value of  $\Delta S$  was calculated as before. The results are given in Table 1.

TABLE 1

Kinetic parameters calculated using the Coats-Redfern (CR), the Freeman-Carroll (FC), Horowitz-Metzger (HM) and the modified Horowitz-Metzger (M-HM) equations

Sample Pb(NO <sub>3</sub> ) <sub>2</sub>	T <sub>i</sub> (°C)		T <sub>s</sub> (°C)		E (kJ mol <sup>-1</sup> )		Z (s <sup>-1</sup> )		ΔS (JK <sup>-1</sup> mol <sup>-1</sup> )							
	380	450	438	450	CR	FC	HM	M-HM	CR	FC	HM	H-HM	CR	FC	HM	M-HM
<i>Stage I</i>																
1 Unirradiated	380	450	438	450	296.8 (0.9997)	324.9 (0.9985)	327.6 (0.9996)	317.8	6.9 × 10 <sup>20</sup>	1.6 × 10 <sup>23</sup>	4.6 × 10 <sup>23</sup>	8.4 × 10 <sup>22</sup>	146.9	191.9	200.9	186.8
2 Irrad 100 Mrad	370	450	437	450	279.3 (0.9972)	305.3 (0.9804)	313.9 (0.9965)	300.7	4.1 × 10 <sup>19</sup>	6.4 × 10 <sup>21</sup>	4.7 × 10 <sup>22</sup>	4.8 × 10 <sup>21</sup>	123.4	164.6	181.1	162.1
3 Irrad 200 Mrad	370	440	427	440	255.6 (0.9985)	263.0 (0.9887)	285.6 (0.9985)	284.7	7.6 × 10 <sup>17</sup>	5.0 × 10 <sup>18</sup>	7.2 × 10 <sup>20</sup>	6.1 × 10 <sup>20</sup>	90.3	105.9	147.3	146.0
4 Irrad 300 Mrad	360	440	425	440	232.7 (0.9976)	231.6 (0.9803)	261.6 (0.9980)	261.9	1.4 × 10 <sup>16</sup>	2.2 × 10 <sup>16</sup>	1.2 × 10 <sup>19</sup>	1.3 × 10 <sup>19</sup>	57.5	60.7	113.4	113.9
5 Irrad 400 Mrad	350	440	423	440	211.4 (0.9972)	223.1 (0.9867)	239.8 (0.9970)	241.6	3.5 × 10 <sup>14</sup>	5.1 × 10 <sup>15</sup>	3.0 × 10 <sup>17</sup>	4.1 × 10 <sup>17</sup>	26.5	48.8	82.5	85.2
<i>Stage II</i>																
1 Unirradiated	450	490	460	490	93.9 (0.9986)	104.0 (0.9979)	103.3 (0.9992)	100.5	3.2 × 10 <sup>5</sup>	4.1 × 10 <sup>6</sup>	2.6 × 10 <sup>6</sup>	1.6 × 10 <sup>6</sup>	-147.0	-125.9	-129.5	-133.5
2 Irrad 100 Mrad	450	490	458	490	91.6 (0.9991)	101.1 (0.9814)	99.3 (0.9986)	100.1	2.2 × 10 <sup>5</sup>	2.7 × 10 <sup>6</sup>	1.4 × 10 <sup>6</sup>	1.7 × 10 <sup>6</sup>	-149.8	-130.1	-135.6	-133.7
3 Irrad 200 Mrad	440	490	457	490	89.1 (0.9973)	99.5 (0.9903)	98.0 (0.9989)	99.5	1.4 × 10 <sup>5</sup>	2.2 × 10 <sup>6</sup>	1.1 × 10 <sup>6</sup>	1.5 × 10 <sup>6</sup>	-153.6	-131.1	-136.4	-134.2
4 Irrad 300 Mrad	440	490	455	490	88.7 (0.9973)	96.6 (0.9983)	95.2 (0.9981)	91.3	1.2 × 10 <sup>5</sup>	1.4 × 10 <sup>6</sup>	1.4 × 10 <sup>6</sup>	3.7 × 10 <sup>5</sup>	-156.1	-134.6	-134.5	-145.8
5 Irrad 400 Mrad	440	490	454	490	86.7 (0.9967)	93.7 (0.9852)	93.9 (0.9968)	87.8	1.1 × 10 <sup>5</sup>	8.6 × 10 <sup>5</sup>	5.9 × 10 <sup>5</sup>	2.0 × 10 <sup>5</sup>	-160.2	-138.7	-141.8	-150.8
<i>Stage III</i>																
1 Unirradiated	560	580	565	580	133.1 (0.9985)	-	140.5 (0.9986)	137.0	3.8 × 10 <sup>7</sup>	-	6.9 × 10 <sup>7</sup>	4.1 × 10 <sup>7</sup>	-108.3	-	-103.5	-107.8
2 Irrad 100 Mrad	555	575	565	575	130.8 (0.9983)	-	138.0 (0.9987)	133.3	3.1 × 10 <sup>7</sup>	-	4.7 × 10 <sup>7</sup>	4.7 × 10 <sup>7</sup>	-110.1	-	-107.4	-107.4
3 Irrad 200 Mrad	550	570	558	570	116.1 (0.9996)	-	132.8 (0.9998)	123.9	3.6 × 10 <sup>7</sup>	-	2.6 × 10 <sup>7</sup>	6.7 × 10 <sup>6</sup>	-128.0	-	-111.5	-122.8
4 Irrad 300 Mrad	550	570	558	570	118.8 (0.9981)	-	130.8 (0.9953)	123.3	6.2 × 10 <sup>6</sup>	-	1.9 × 10 <sup>7</sup>	3.8 × 10 <sup>6</sup>	-123.4	-	-114.1	-127.4
5 Irrad 400 Mrad	550	565	555	565	114.7 (0.9996)	-	130.6 (0.9998)	118.8	2.5 × 10 <sup>6</sup>	-	1.2 × 10 <sup>7</sup>	3.6 × 10 <sup>6</sup>	-130.9	-	-118.8	-127.9

The data were also analysed using the Horowitz–Metzger equation as modified by Dharwadkar and Karakhanavala [15] For a first-order process, the equation is used in the form

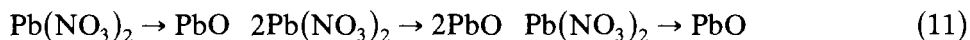
$$\log[\log(1 - \alpha)^{-1}] = 100E\theta/2.3RT_i^2(T_f - T_i) - \log 2.3 \quad (10)$$

where  $T_i$  is the temperature of inception of the reaction and  $T_f$  is the temperature of completion of the reaction  $R$  is the gas constant A plot of the left-hand side of eqn (10) versus  $\theta$  was linear for the three stages as required by the theory, and  $E$  was calculated from the slope Values of  $Z$  and  $\Delta S$  were calculated as before The results of the analysis are given in Table 1

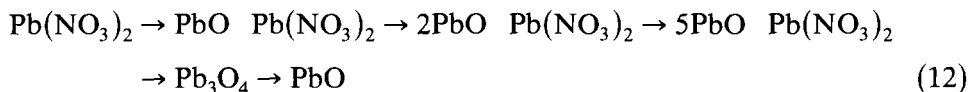
The  $E$  and  $Z$  values obtained by means of the four methods show that the agreement between these methods is good (within about 12%) However,  $\Delta S$  values by these methods show some variations For the third stage, comparable values for  $E$  were not obtained by the Freeman–Carroll method These values are not given in Table 1

## DISCUSSION

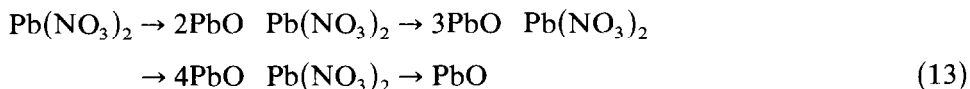
Baekeland [1] has reported that the decomposition of lead nitrate begins at 205°C and becomes energetic above 357°C and proceeds by the following stages



Nicol [2] has suggested the following decomposition procedure



Vratny [4] reported that the decomposition proceeds via a basic nitrate or metallic nitrite structure Thermogravimetric studies by Wendlandt [3] show that the decomposition begins at 370°C in air and  $\text{Pb}_2\text{O}(\text{NO}_3)_2$  is formed at the break in the curve at 435°C Jacob et al [6] have observed the decomposition starting at 335°C at the heating rate of 1°C min<sup>-1</sup> in nitrogen atmosphere Margulis et al [5] have found using DTA and TGA studies that the decomposition begins at 380°C and occurs in four stages In the first stage a liquid phase is formed which is due to the formation of a eutectic mixture between  $\text{Pb}(\text{NO}_3)_2$  and 2PbO  $\text{Pb}(\text{NO}_3)_2$ , with  $m_p$  407°C The decomposition proceeds by the stages



As we were interested only in the study of the kinetics of the decomposition, no effort was made to isolate and characterize the products of the individual stages

In the present investigation the decomposition starts at 380°C for the unirradiated salt. The reaction is found to occur in three stages. After the first stage, a break is observed in the TG curve similar to that observed by Wendlandt [3]. The break is very prominent in the unirradiated salt. After the second stage, a horizontal level extending to about 50°C is noticed which was not observed by others. After this level, a very short stage of decomposition is observed which is completed within 20°C.

Irradiation lowers  $T_1$ ,  $T_s$  and  $T_f$  of the three stages (Table 1). For the first stage,  $T_1$  is lowered by 10°C in the samples irradiated with 100 and 200 Mrad and by 20 and 30°C in samples irradiated with 300 and 400 Mrad  $\gamma$ -rays, respectively. For the second and third stages  $T_1$  is lowered only by 10°C.  $T_s$  is lowered by 15, 6 and 10°C for the first, second and third stages, respectively.  $T_f$  is lowered by 15°C. Thus, the effect of irradiation is to lower the values of  $T_1$ ,  $T_f$  and  $T_s$ , as has been observed previously [16,17]. The horizontal level is shortened by 10°C.

The reaction obeys first-order kinetics in the three stages. For the acceleratory stage, the values of  $E$  for the decomposition of unirradiated  $\text{Pb}(\text{NO}_3)_2$  and  $\text{Pb}(\text{NO}_3)_2$  irradiated with 100 and 400 Mrad  $^{60}\text{Co}$   $\gamma$ -rays obtained earlier by the gas evolution method [7] are 251.5, 263.2 and 230.5 kJ, respectively. For the decay stage,  $E$  values reported are 49.0, 59.8 and 68.6 kJ for unirradiated, irradiated with 100 and 400 Mrad, respectively. In the present study, the  $E$  values in some cases are slightly higher than these values. Moreover, the  $E$  values for the second stage show a slight decrease instead of an increase as observed in the gas evolution method. Since  $E$  values for the three stages decrease only to a small extent with increase in irradiation dose, it can be concluded that the same chemical processes govern the decomposition of both the unirradiated and the irradiated salt.

$\gamma$ -Irradiation produces excitation and ionization of the compound anion  $\text{NO}_3^-$  [18]. The excitation and ionization of the anion, however, cause chemical damage in the crystal matrix. The presence of these damaged species in the crystal matrix will result in a steady accumulation of strain. At a temperature sufficient to produce decomposition, this strain may induce rupture in the crystals. The nuclei present before or formed during irradiation grow accordingly and the rate of the thermal decomposition is enhanced. Thus, the fall in the initial horizontal level in the case of  $\gamma$ -irradiated samples can be attributed to the effect of irradiation.

The primary radiolytic fragments produced in the radiolysis of nitrate are  $\text{NO}_2^-$  and O. The radiolytic oxygen becomes trapped in the crystal lattice. As the temperature is increased, annealing of the damage  $\text{NO}_2^-$  takes place [18]. In the initial part of the first stage, the lowering of  $E$  may be due to the presence of the crystal defects (Table 1). At this stage, although there is

chance of a considerable decrease in the  $\text{NO}_2^-$  at such a high temperature, a part of  $\text{NO}_2^-$  remains unannealed. This is evident from the fraction annealed ( $\phi = 0.9$ ) at  $230^\circ\text{C}$  when irradiated  $\text{Pb}(\text{NO}_3)_2$  is heated for 100 h [19]. The  $\text{NO}_2^-$  which remains unannealed catalyses the decomposition. Moreover, since a liquid phase as reported by Margulis [5] is formed at the first stage, a large proportion of the damage oxygen escapes leaving behind a portion of  $\text{NO}_2^-$ . The  $\text{NO}_2^-$  which remains unannealed catalyses the decomposition. The catalysing effect of  $\text{NO}_2^-$  on the thermal decomposition of nitrates has also been established earlier [20].

For the second stage, the  $E$  value is only slightly decreased (Table 1). This may be because most of the defects are removed by annealing and the eutectic phase formation. However, the decrease is due to  $\text{NO}_2^-$  that escaped annealing in the first stage.

In the third stage, the  $E$  value is less than that in the second stage. This can be attributed to the  $\text{PbO}$  formed which can act as an additional catalysing agent.

The values of  $\Delta S$  also decrease in the three stages.

#### *Mechanism of reaction from non-isothermal TG traces*

The non-isothermal kinetic methods discussed by Šesták and Berggren [21] and Satava [22], have been used for deducing the mechanism of

TABLE 2

Kinetic parameters calculated using the mechanism-based equation,  $-\ln(1-\alpha) = kt$

Parameter	$\text{Pb}(\text{NO}_3)_2$	$\text{Pb}(\text{NO}_3)_2$ irradiated with			
		100 Mrad	200 Mrad	300 Mrad	400 Mrad
<i>Stage I</i>					
Slope	-37 01314	-34 95427	-32 08927	-29 33547	-26 76496
Intercept	51 67556	48 97825	45 03182	41 17437	37 52458
$r$	0 99981	0 99747	0 99866	0 99783	0 99750
$E$ (kJ mol <sup>-1</sup> )	318.6	301.3	277.3	254.3	232.7
$Z$ (s <sup>-1</sup> )	$2.8 \times 10^{22}$	$1.9 \times 10^{21}$	$3.6 \times 10^{19}$	$7.6 \times 10^{17}$	$2.0 \times 10^{16}$
<i>Stage II</i>					
Slope	-12 77418	-12 52076	-12 00297	-11 91188	-11 76948
Intercept	17 64973	17 34583	16 70479	16 61862	16 46707
$r$	0 99891	0 99942	0 99854	0 99792	0 99708
$E$ (kJ mol <sup>-1</sup> )	115.6	113.5	109.1	108.4	107.2
$Z$ (s <sup>-1</sup> )	$4.6 \times 10^7$	$3.4 \times 10^7$	$1.8 \times 10^7$	$1.6 \times 10^7$	$1.4 \times 10^7$
<i>Stage III</i>					
Slope	-17 66843	-16 43538	-15 63839	-15 93663	-15 44545
Intercept	22 34599	21 00040	20 09817	20 60383	19 97852
$r$	0 99876	0 99911	0 99972	0 99850	0 99972
$E$ (kJ mol <sup>-1</sup> )	156.6	146.3	139.6	142.1	138.0
$Z$ (s <sup>-1</sup> )	$5.1 \times 10^9$	$1.3 \times 10^9$	$5.6 \times 10^8$	$8.9 \times 10^8$	$4.7 \times 10^7$



decomposition of  $\text{Pb}(\text{NO}_3)_2$ . The computational approach to obtain the correct mechanism and the corresponding  $E$  and  $Z$  values has already been discussed [16]. For the correct mechanism,  $\ln g(\alpha)$  versus  $1/T$  should be a straight line. The functional values of  $\ln g(\alpha)$  required for this purpose were taken from the table of Nair and James [23] and  $E$  was calculated by the method of Šesták [24] from the slope. For almost the same value of  $\nu$ , the operating mechanism was chosen by comparing the  $E$  values with those obtained by the non-mechanistic equation. It is found that the  $F_1$  mechanism gives the maximum correlation for the three stages in all cases (Table 2). Therefore the decomposition of  $\text{Pb}(\text{NO}_3)_2$ , both unirradiated and irradiated, follows the Mampel model equation [25], viz  $-\ln(1 - \alpha)$  for  $g(\alpha)$  in each stage, and the rate-controlling process is random nucleation with the formation of a nucleus on every particle. Since the values of  $E$  and  $Z$  computed from the mechanism-based equation agree well with those from the mechanism-non-invoking approach, this mechanism is confirmed.

## REFERENCES

- 1 L Baekeland, *J Am Chem Soc*, 26 (1904) 391
- 2 A Nicol, *C R Acad Sci*, 226 (1948) 253
- 3 W W Wendlandt, *Texas J Sci*, 10 (1958) 392
- 4 F Vratny and F Gugliotta, *J Inorg Nucl Chem* 25 (1963) 1129
- 5 E V Margulis, M M Shokarev, L A Savchenko, L I Beisekeeva and F I Vershinina, *Russ J Inorg Chem*, 17(1) (1972) 21
- 6 J Mu and D D Perlmutter, *Thermochim Acta*, 56 (1982) 253
- 7 S R Mohanty and M N Ray, *Indian J Chem*, 6(6) (1968) 319
- 8 C H Bamford and C F H Tipper, *Comprehensive Chemical Kinetics*, Vol 22, Elsevier, Amsterdam, 1980
- 9 P M D Benoit, R G Ferrillo and A H Granzow, *J Therm Anal*, 30 (1985) 869
- 10 W W Wendlandt, *Thermal Methods of Analysis*, Wiley, New York, 2nd edn, 1974, p 45
- 11 S M K Nair and Koshy Kunju Malayil, *J Radio Anal Nucl Chem Lett*, 96 (1985) 521
- 12 A W Coats and J P Redfern, *Nature (London)*, 201 (1964) 68
- 13 E S Freeman and B Carroll, *J Phys Chem*, 62 (1958) 394
- 14 H H Horowitz and G Metzger, *Anal Chem*, 35 (1963) 1464
- 15 S R Dharwadkar and M D Karakhanavala, in R F Schwenker, Jr and P D Garn (Eds) *Thermal Analysis*, Vol 2, Proc 2nd ICTA, Worcester, MA, 1968, Academic Press, New York, 1969, p 1049
- 16 S M K Nair and C James, *Thermochim Acta*, 78 (1984) 357
- 17 S M K Nair and C James, *Thermochim Acta*, 96 (1985) 27
- 18 S R Mohanty and V M Pandey, *J Sci Ind Res*, 34 (1975) 196
- 19 S R Mohanty and S M K Nair, *Indian J Chem*, 8 (1970) 158
- 20 S M K Nair and C James, *Thermochim Acta*, 87 (1985) 367
- 21 J Šesták and G Berggren, *Thermochim Acta*, 3 (1971) 1
- 22 V Satava, *Thermochim Acta*, 2 (1971) 423
- 23 S M K Nair and C James, *Thermochim Acta*, 83 (1985) 387
- 24 J Šesták, *Thermochim Acta*, 3 (1971) 150
- 25 K L Mampel, *Z Phys Chem Abt A*, 187 (1940) 235